Polymer Chemistry

RSC Publishing

COMMUNICATION

View Article Online
View Journal | View Issue

A new insight into the *in situ* thermal reduction of graphene oxide dispersed in a polymer matrix†

Cite this: *Polym. Chem.*, 2013, **4**, 1765

Shibing Ye and Jiachun Feng*

Received 5th January 2013
Accepted 30th January 2013

DOI: 10.1039/c3py00019b

www.rsc.org/polymers

By comparing the reduction temperatures of graphene oxide dispersed in non-polar, polar and aromatic polymers, we proposed a mechanism that the interactions between graphene oxide and polymers play a key role in decreasing the reduction temperature of graphene oxide dispersed in a polymer matrix.

Graphene holds promising applications in polymer composites due to its large aspect ratio, outstanding mechanical properties, good thermal stability and high electrical conductivity.[1–4] Considering the strong aggregation of graphene sheets in various polymer matrices, graphene oxide (GO) is commonly used as the starting material in place of graphene.[5–9] In practice, GO is also a potential filler for polymer composites for its large aspect ratio and high mechanical strength. Moreover, in view of its abundant oxygen-containing groups, GO shows a more effective reinforcement effect than graphene for polar polymers like polyvinyl alcohol and polymethyl methacrylate (PMMA).[10–12] However, it is noteworthy that, whether polymer/graphene or polymer/GO is produced with GO as the starting material, the resulting nanocomposites have to undergo melt processing before preparing specimens for mechanical measurements or manufacturing products for applications.[7,9,11,13,14] This highly scalable and environmentally friendly processing technique will inevitably lead to the reduction of GO in a polymer matrix, which has been reported in some earlier works.[7–9,13] For instance, polyvinylidene fluoride/GO (PVDF/GO) could be thermally reduced to PVDF/graphene by hot pressing the former at 200 °C for 2 h.[7] Recently, in a milestone work,[15] Glover and Schniepp *et al.* found that GO dispersed in various polymer matrices shows different reduction temperatures (RTs) and reduction degrees. Then, a "big" question naturally arises, that is, what is really responsible for the change of the reduction behavior of GO? Until now, to the best of our knowledge, no further study has been done to systematically reveal the effect of polymer matrices' chemistry on the *in situ* thermal reduction of GO. Addressing this question will help us understand the nature of the *in situ* thermal reduction of GO in a polymer matrix and be of great interest in both academic and industrial research.

In this work, through choosing some typical polymers with different structures and polarities, we first investigated the effect of polymer matrices' chemistry on the reduction behavior of GO in a polymer matrix from the perspective of their interactions. Non-polar octene-ethylene copolymer (POE), aromatic polystyrene (PS) and poly (styrene-*b*-(ethylene-*co*-butylene)-*b*-styrene) (SEBS), polar PMMA and ethylene-vinyl acetate copolymer (EVA) were selected as matrices of the nanocomposites. Typically, the polymer/GO nanocomposites containing 10 wt% GO sheets were synthesized by a solution-casting method (The chemical structural formulae of polymers used and the experimental details can be found in the ESI†). The X-ray diffraction (XRD) patterns (Fig. 1a) of polymer/GO nanocomposites exhibit sharp peaks, which indicate that the GO sheets still pack into an

State Key Laboratory of Molecular Engineering of Polymers, Department of Macromolecular Science, Fudan University, Shanghai 200433, P. R. China. E-mail: jcfeng@fudan.edu.cn

† Electronic supplementary information (ESI) available: Experimental section; TGA curves of various polymer/GO nanocomposites; XRD and DSC results for PMMA/GO nanocomposites with different GO concentrations; FESEM images of the fracture surfaces of SEBS/GO and PMMA/GO treated at different temperatures; XRD patterns and Raman spectra of PMMA/GO and SEBS/GO treated at different temperatures; TGA curves and Raman spectra of GO, X-RGO and O-RGO; DSC curves for polyacrylamide (PAM)/GO nanocomposites; TGA and DSC data for various nanocomposites. See DOI: 10.1039/c3py00019b

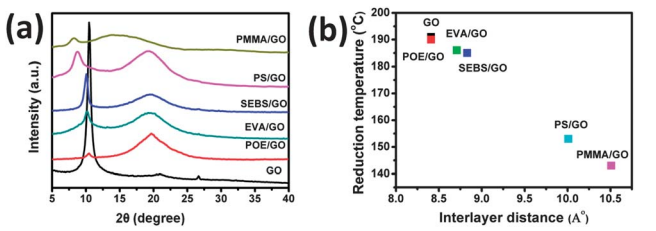

Fig. 1 (a) XRD patterns of GO and polymer/GO nanocomposites, (b) decrease of the RT of GO with the increase of the interlayer distance.

ordered structure in polymer matrices. Compared to pure GO, the typical diffraction peak of GO ($2\theta = 10.5°$) shifts to lower angles when incorporated into polymer matrices, indicating larger interlayer distances. This could be attributed to the intercalation of polymer chains into the interlayers of GO sheets. Surprisingly, the interlayer distances of GO vary with different polymers, which may be explained by the distinctly different interactions that polymers would have with GO sheets.[16] For example, polar PMMA, with numerous carbonyl groups, would likely interact well with the surface of GO *via* hydrogen bonding, leading to intercalation between GO sheets and resulting in a large increase of the interlayer distance. Similarly, aromatic PS would play the same role in the change of the interlayer distance of GO *via* π–π stacking.

The RTs of GO in nitrogen and various polymer matrices were determined by differential scanning calorimetry (DSC), an effective technique to evaluate the reduction behavior of GO.[8,15] Here, the temperature at the maximum of the endothermic peak in the DSC curve was defined as the RT of GO. As shown in Fig. 2a, the DSC thermogram of GO in nitrogen exhibits a strong exothermic peak at 191 °C with a heat release of 1275 J g^{-1}, which should be attributed to the thermal reduction of GO. Fortunately, from the DSC thermograms in Fig. 2b, c and d, no apparent thermal signals are observed for all the neat polymers we used within the investigated temperature range of 100–250 °C. The single exothermic peak that appears in the DSC thermogram of the polymer/GO nanocomposite can be certainly attributed to the *in situ* reduction of GO dispersed in the polymer matrix. Fig. 2b shows only a slight decrease (1 °C) of the RT in the POE matrix, indicating that the non-polar POE imparts negligible influence on the RT of GO. For polar polymers, the RT slightly shifts to 186 °C when GO is dispersed in EVA, while heavily decreases to 142 °C when it is dispersed in PMMA (Fig. 2c), suggesting that the presence of PMMA decreases the RT of GO more remarkably than EVA does. Similarly, for aromatic polymers, GO in PS shows a significant decrease in RT from 191 to 153 °C, while GO in SEBS shows a weak decrease in RT from 191 to 185 °C (Fig. 2d), suggesting that the former makes GO reduce more easily than the latter. Thermogravimetric analysis (TGA) also reveals the same tendency for the changes of the RT (Fig. S2, ESI†), and the detailed information of both DSC and TGA is listed in Table S1.† It is noteworthy that, combined with the XRD results, it seems that the decreasing RT of GO is correlated with the increasing interlayer distance of GO for these polymer/GO nanocomposites (Fig. 1b). A similar tendency was also observed in the polymer/GO nanocomposites with different GO concentrations (Fig. S3, ESI†). This narrow correlation suggests that the larger the interlayer distance GO has, the lower the RT GO needs.

Generally, reduction of GO in polymer nanocomposites affects their macroscopic performance such as mechanical and electrical properties. To further confirm the RT of GO corresponding to each polymer, a comparative study of electrical conductivity was done. Electrical conductivities for two representative samples that underwent thermal treatment at different temperatures were measured. According to the DSC results, 150 °C is chosen as the first treating temperature, which is between the RTs of GO in PMMA and SEBS, while 195 °C is chosen as the second treating temperature, which is higher than the RTs of GO in both the above polymers. Since both GO and polymers used in this work are insulators, electrical conductivities of polymer/GO nanocomposites could conceivably reflect the reduction degree of GO.[7,8,15] As shown in Fig. 3, the PMMA/GO nanocomposite thermally treated at 150 °C for 4 h has a high electrical conductivity of 0.72 S m^{-1}, while the SEBS/GO nanocomposite treated under identical conditions shows a rather low electrical conductivity (<10^{-2} S m^{-1}). This enormous difference in electrical conductivity indicates that the reduction degree of GO in PMMA is much higher than that in SEBS at a temperature of 150 °C. By increasing the treating temperature to 195 °C, the conductivity of the PMMA/GO nanocomposite approaches to 0.94 S m^{-1}, meanwhile, the SEBS/GO nanocomposite also yields an increase in electrical conductivity with a final value of 0.34 S m^{-1}. The relatively high electrical conductivity indicates that GO dispersed in both PMMA and SEBS possesses high reduction degrees at a treating temperature of 195 °C. More information could be obtained by comparing the electrical conductivity horizontally. As for the PMMA/GO nanocomposite, the slightly increased electrical

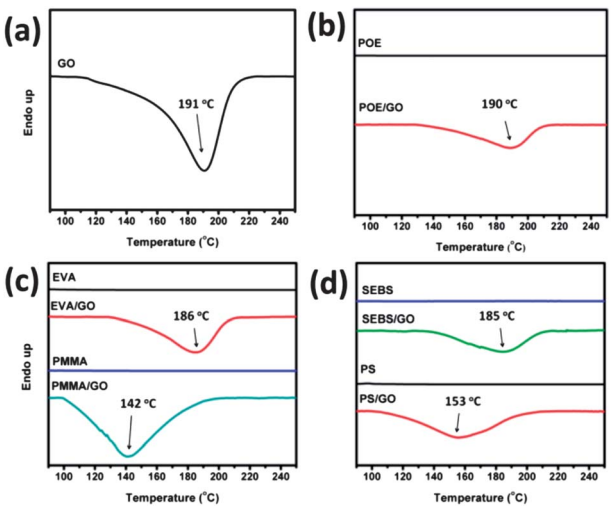

Fig. 2 DSC curves of (a) GO, (b) POE and POE/GO, (c) EVA, PMMA, EVA/GO and PMMA/GO, (d) SEBS, PS, SEBS/GO and PS/GO.

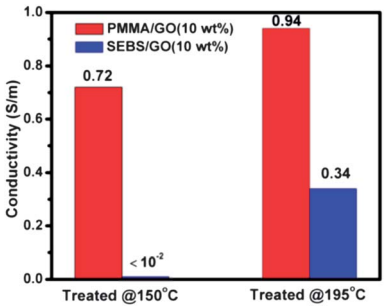

Fig. 3 Electrical conductivities of PMMA/GO and SEBS/GO nanocomposites thermally treated at 150 and 195 °C for 4 h, respectively.

conductivity from 0.72 to 0.94 S m^{-1} implies that, once above its RT, GO reduction degree increases slowly by increasing the temperature from 150 to 195 °C. In contrast, as for the SEBS/GO nanocomposite, the electrical conductivity shows a dramatic increase from $<10^{-2}$ to 0.34 S m^{-1} by several orders of magnitude, strongly suggesting that 195 °C, above the RT of GO in SEBS (185 °C), is sufficient to reduce GO, reconstructing the conduction pathways, but 150 °C, below its RT, is not. Simultaneously, GO reduction changes the surface chemistry of GO,[17] which will affect the compatibility of GO sheets with the polymer matrix (The morphologies of the fracture surface of the nanocomposites are shown in Fig. S4 in the ESI†). Therefore, the electrical conductivity data not only confirm the "new" RTs of GO in polymer matrices, consistent with the DSC results, but also underline the importance of processing temperature in tailoring the morphologies and performance of polymer/GO nanocomposites.

The three parallel experiments described above make it clear that GO incorporated in polar and aromatic polymer matrices thermally reduce at lower temperatures than GO incorporated in a non-polar polymer matrix, which shows a similar RT to pristine GO. For PS/GO nanocomposites, the presence of aromatic PS decreases the RT of GO by 38 °C. Previous reports showed that aromatic solvents have a similar decrease effect on the RT of GO.[18,19] Barroso-Bujans *et al.*[18] illustrated that aromatic solvents such as benzene, toluene, and *p*-xylene adsorbed in the interlayers of GO significantly decrease the RT of GO (the reduction of GO in xylene and octane has been conducted to evidence the influence of the benzene ring, which is shown in Fig. S6, ESI†). Given the same structure of the phenyl ring in the polymer and solvents, we speculate that there also exists a close relationship between phenyl rings and the decrease of RT. This may be further confirmed by the results of the SEBS/GO nanocomposite. The minor decrease (6 °C) of RT should be ascribed to the only 31% content of styrene segments in the present SEBS. In the case of polar polymer series, GO in PMMA, containing plentiful polar ester groups, is reduced at a low temperature with a great decrease of 49 °C. Zhu *et al.*[20] found that GO dispersed in propylene carbonate, a highly polar cyclic ester, can be significantly reduced at a moderate temperature of 150 °C. Therefore, we believe that these polar ester groups play a key role in decreasing the RT of GO. Similarly, with respect to the EVA/GO nanocomposite, a consistent result demonstrates that the RT of GO in EVA, that contains only 24% polar VAc segments, shows a smaller decrease of 5 °C. To verify the influence of a polar polymer on GO reduction, the RT of GO in polyacrylamide, another strongly polar polymer, was also measured (Fig. S7 in the ESI†). It is found that the RT in this nanocomposite is 155 °C, largely lower than that of pure GO, which coincides with the results of the above polar polymers.

So far, rarely has work focused on the reduction mechanisms of GO in a polymer matrix due to the lack of means to directly monitor reduction processes and the complexity of chemical reactions.[21] Based on the limited results of this exploratory study, a possible mechanism can be deduced in which the decrease of RT is related to the interactions between GO sheets and the polymer matrix. Fig. 4 schematically illustrates the role of favorable interactions between GO sheets and polymer matrices in the *in situ* thermal reduction of GO. In a typical model proposed by Rourke *et al.*,[22] GO is presented as the combination of large graphene sheets and oxidative debris in which the oxidative debris is strongly adhered to the graphene sheet through π–π stacking or van der Waals interactions (Fig. 4a).[23] As shown in Fig. 4b, for the aromatic polymers (*e.g.* PS), they adsorb on the surface of graphene sheets through π–π stacking, which is formed between the continuous phenyl rings and the conjugated basal planes of graphene.[24,25] The favorable interactions facilitate the intercalation of aromatic polymer chains into the interlayers of GO, resulting in an increase of the intersheet spacing of GO sheets,[16] which is in accordance with the XRD results (Fig. 1a). When the interactions between aromatic polymers and graphene sheets are strong enough to counterbalance the interactions between graphene sheets and oxidative debris, this strong adhesion of polymers will make some of the oxidative debris leave the graphene sheets and render them free during the melt heating process. Both the relatively larger intersheet spacing and free oxidative debris lead to the reduction of GO requiring lower energy, and consequently lower RT (Fig. 4c). For the polar polymers (*e.g.* PMMA), the abundant polar groups allow

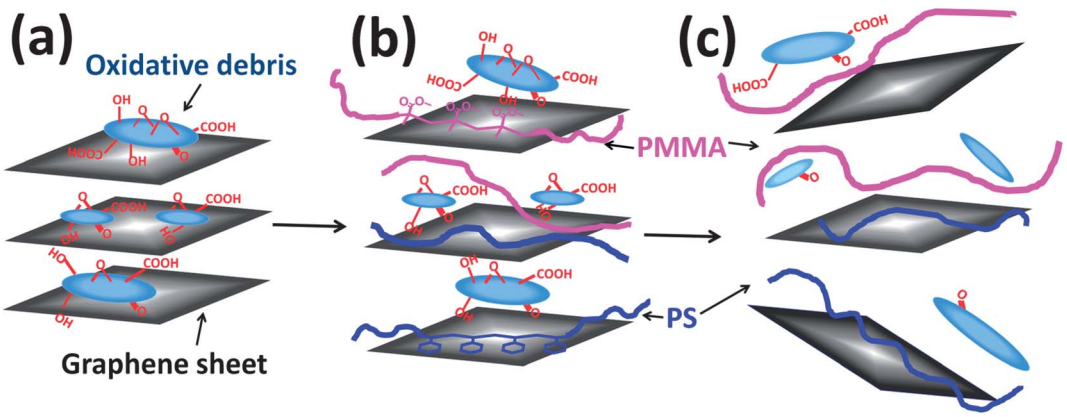

Fig. 4 Schematic illustration of the GO model and the interaction between GO and polymers.

for the formation of hydrogen bonding with oxidative debris.[11,12] With the aid of hydrogen bonding interaction, polar polymers not only intercalate into the interlayers of GO, but also peel off oxidative debris from the graphene sheet, which also produce a large intersheet distance of GO and free oxidative debris (Fig. 4b). As a result, GO in polar polymer matrices could be reduced at relatively lower RTs. As a non-polar polymer, POE almost does not decrease the RT of GO because it does not have any interactions with GO, which in turn supports our proposed mechanism.

Conclusions

In summary, this work systematically investigates the influence of polymer matrices' chemistry on the *in situ* thermal reduction of GO dispersed in a polymer matrix. Interestingly, both polar polymers and aromatic polymers can decrease the RT of GO but non-polar polymers cannot. The limited data convince us that the change in the RT of GO is associated with the favorable interactions between polymers and GO sheets. Although this study merely touches a tiny part of the *in situ* thermal reduction of GO in the polymer matrix, the present results will provide a scientific reference for choosing suitable processing temperatures and proper polymers to optimize the performance of polymer/GO nanocomposites in industrial production.

Acknowledgements

This work was financially supported by the Natural Science Foundation of China (21174032), the National Basic Research Program of China (2011CB605704) and PetroChina Innovation Foundation (2011D50060504).

Notes and references

1 Y. W. Zhu, S. Murali, W. W. Cai, X. S. Li, J. W. Suk, J. R. Potts and R. S. Ruoff, *Adv. Mater.*, 2010, **22**, 3906.
2 X. Huang, Z. Y. Zeng, Z. X. Fan, J. Q. Liu and H. Zhang, *Adv. Mater.*, 2012, **24**, 5979.
3 X. Huang, X. Y. Qi, F. Boey and H. Zhang, *Chem. Soc. Rev.*, 2012, **41**, 666.
4 X. Huang, Z. Y. Yin, S. X. Wu, X. Y. Qi, Q. Y. He, Q. C. Zhang, Q. Y. Yan, F. Boey and H. Zhang, *Small*, 2011, **7**, 1876.
5 X. Y. Qi, K. Y. Pu, H. Li, X. Z. Zhou, S. X. Wu, Q. L. Fan, B. Liu, F. Boey, W. Huang and H. Zhang, *Angew. Chem., Int. Ed.*, 2010, **49**, 9426.
6 X. Y. Qi, K. Y. Pu, X. Z. Zhou, H. Li, B. Liu, F. Boey, W. Huang and H. Zhang, *Small*, 2010, **6**, 663.
7 H. X. Tang, G. J. Ehlert, Y. R. Lin and H. A. Sodano, *Nano Lett.*, 2012, **12**, 84.
8 M. Traina and A. J. Pegoretti, *J. Nanopart. Res.*, 2012, **14**, 1.
9 N. Wu, X. L. She, D. J. Yang, X. F. Wu, F. B. Su and Y. F. Chen, *J. Mater. Chem.*, 2012, **22**, 17254.
10 C. L. Bao, Y. Q. Guo, L. Song and Y. Hu, *J. Mater. Chem.*, 2011, **21**, 13942.
11 J. R. Potts, S. H. Lee, T. M. Alam, J. An, M. D. Stoller, R. D. Piner and R. S. Ruoff, *Carbon*, 2011, **49**, 2615.
12 T. Ramanathan, A. A. Abdala, S. Stankovich, D. A. Dikin, M. Herrera-Alonso, R. D. Piner, D. H. Adamson, H. C. Schniepp, X. Chen, R. S. Ruoff, S. T. Nguyen, I. A. Aksay, R. K. Prud'homme and L. C. Brinson, *Nat. Nanotechnol.*, 2008, **3**, 327.
13 W. J. Li, X. Z. Tang, H. B. Zhang, Z. G. Jiang, Z. Z. Yu, X. S. Du and Y. W. Mai, *Carbon*, 2011, **49**, 4724.
14 J. R. Potts, S. Murali, Y. W. Zhu, X. Zhao and R. S. Ruoff, *Macromolecules*, 2011, **44**, 6488.
15 A. J. Glover, M. Z. Cai, K. R. Overdeep, D. E. Kranbuehl and H. C. Schniepp, *Macromolecules*, 2011, **44**, 9821.
16 K. W. Putz, O. C. Compton, M. J. Palmeri, S. T. Nguyen and L. C. Brinson, *Adv. Funct. Mater.*, 2010, **20**, 3322.
17 H. B. Zhang, W. G. Zheng, Q. Yan, Z. G. Jiang and Z. Z. Yu, *Carbon*, 2012, **50**, 5117.
18 F. Barroso-Bujans, S. Cerveny, R. Verdejo, J. J. del Val, J. M. Alberdi, A. Alegria and J. Colmenero, *Carbon*, 2010, **48**, 1079.
19 D. R. Dreyer, S. Murali, Y. W. Zhu, R. S. Ruoff and C. W. Bielawski, *J. Mater. Chem.*, 2011, **21**, 3443.
20 Y. W. Zhu, M. D. Stoller, W. W. Cai, A. Velamakanni, R. D. Piner, D. Chen and R. S. Ruoff, *ACS Nano*, 2010, **4**, 1227.
21 S. F. Pei and H. M. Cheng, *Carbon*, 2012, **50**, 3210.
22 J. P. Rourke, P. A. Pandey, J. J. Moore, M. Bates, I. A. Kinloch, R. J. Young and N. R. Wilson, *Angew. Chem., Int. Ed.*, 2011, **50**, 3173.
23 A. F. Faria, D. S. T. Martinez, A. C. M. Moraes, M. da Costa, E. B. Barros, A. G. Souza, A. J. Paula and O. L. Alves, *Chem. Mater.*, 2012, **24**, 4080.
24 Y. W. Cao, J. Zhang, J. C. Feng and P. Y. Wu, *ACS Nano*, 2011, **5**, 5920.
25 B. Shen, W. T. Zhai, C. Chen, D. D. Lu, J. Wang and W. G. Zheng, *ACS Appl. Mater. Interfaces*, 2011, **3**, 3103.

